

# Superresolution optical system by common-path interferometry

Vicente Mico

*AIDO, Instituto Tecnológico de Óptica, Color e Imagen. C/ Nicolás Copérnico, 7-13  
Parc Tecnològic - 46980 Paterna (Valencia) Spain*

Zeev Zalevsky

*School of Engineering, Bar-Ilan University, Ramat-Gan, 52900 Israel*

Javier Garcia

*Departamento de Optica, Universitat de Valencia. C/Dr.Moliner,50. 46100 Burjassot, Spain  
[javier.garcia.monreal@uv.es](mailto:javier.garcia.monreal@uv.es)*

**Abstract:** We present a new approach to obtain superresolved images in digital holography by means of synthetic aperture generation using common-path interferometry and off-axis illumination in optical imaging systems. The paper includes two parts. First, we present a simple approach to double the resolution of an optical system using tilted illumination onto the object and an optical element in the image plane to produce the holographic recording. Then we present a novel approach consisting of attaching a diffraction grating in parallel together with the object in the input plane and using off-axis illumination provided by a Vertical Cavity Surface Emitting Lasers (VCSEL) array to allow us achieving a major improvement in the optical resolution limit with an extremely low penalty in the complexity of the resulting system. Experimental investigation based on commercial microscope objectives is presented.

©2004 Optical Society of America

**OCIS codes:** (100.6640) Superresolution; (100.0100) Image processing; (110.0110) Imaging systems; (100.2000) Digital image processing; (090.0090) Holography

---

## References and links

1. D. Courjon, *Near-Field Microscopy and Near-Field Optics* (Imperial College Press, London, 2003).
2. M. G. L. Gustafsson, "Nonlinear structured-illumination microscopy: wide-field fluorescence imaging with theoretically unlimited resolution," *Proc. Natl. Acad. Sci. USA* **102**, 13081-13086 (2005).
3. Z. Zalevsky and D. Mendlovic, *Optical Super Resolution*, (Springer 2002).
4. Z. Zalevsky, D. Mendlovic, and A. W. Lohmann, "Optical systems with improved resolving power," *Prog. Opt.*, **40**, 271-341 (1999).
5. G. Toraldo di Francia, "Resolving power and information," *J. Opt. Soc. Am. A* **45**, 497-501 (1955).
6. G. Toraldo di Francia, "Degrees of freedom of an image," *J. Opt. Soc. Am.* **59**, 799-804 (1969).
7. I. J. Cox and J. R. Sheppard, "Information capacity and resolution in an optical system," *J. Opt. Soc. Am. A* **3**, 1152-1158 (1986).
8. P. H. Van Cittert, "Zum einfluss der spaltbreite auf die intensitätsverteilung in spektrallinien," *Z. Physik* **69**, 298-308 (1931).
9. R. W. Gerchberg, "Superresolution through error energy reduction," *Opt. Acta* **21**, 709-720 (1974).
10. W. Lukosz, "Optical systems with resolving powers exceeding the classical limits II," *J. Opt. Soc. Am* **57**, 932-941 (1967).
11. M. A. Grimm and A. W. Lohmann, "Superresolution image for one-dimensional object," *J. Opt. Soc. Am.* **56**, 1151-1156 (1966).
12. A. Shemer, D. Mendlovic, Z. Zalevsky, J. Garcia, and P. Garcia-Martinez, "Superresolving optical system with time multiplexing and computer decoding," *Appl. Opt.* **38**, 7245-7251 (1999).
13. M. G. L. Gustafsson, A. Agard, and W. Sedat, "I<sup>5</sup>M: 3D widefield light microscopy with better than 100 nm axial resolution," *J. Microsc.* **195**, 10-16 (1999).

14. M. Françon, "Amélioration de la résolution d'optique," *Il Nuovo Cimento Suppl.* **9**, 283-290 (1952).
15. A. W. Lohmann and D. P. Paris, "Superresolution for nonbirefringent objects," *Appl. Opt.* **3**, 1037-1043 (1964).
16. A. Zlotnik, Z. Zalevsky, and E. Marom, "Superresolution with nonorthogonal polarization coding," *Appl. Opt.* **44**, 3705-3715 (2005).
17. A. I. Kartashev, "Optical system with enhanced resolving power," *Opt. Spectra.* **9**, 204-206 (1960).
18. A. Shemer, Z. Zalevsky, D. Mendlovic, N. Konforti, and E. Marom, "Time multiplexing superresolution based on interference grating projection," *Appl. Opt.* **41**, 7397-7404 (2002).
19. V. Mico, Z. Zalevsky, P. García-Martínez, and J. García, "Single step superresolution by interferometric imaging," *Opt. Express* **12**, 2589-2596 (2004).
20. X. Chen and S. R. J. Brueck, "Imaging interferometric lithography: approaching the resolution limits of optics," *Opt. Lett.* **24**, 124-126 (1999).
21. C. J. Schwarz, Y. Kuznetsova, and S. R. J. Brueck, "Imaging interferometric microscopy," *Opt. Lett.* **28**, 1424-1426 (2003).
22. E. N. Leith, D. Angell, and C.-P. Kuei, "Superresolution by incoherent-to-coherent conversion," *J. Opt. Soc. Am. A*, **4**, 1050-1054 (1987).
23. P. C. Sun and E. N. Leith, "Superresolution by spatial-temporal encoding methods," *Appl. Opt.* **31**, 4857-4862 (1992).
24. V. Mico, Z. Zalevsky, P. García-Martínez, and J. García, "Superresolved imaging in digital holography by superposition of tilted wavefronts," *Appl. Opt.* **45**, 822-828 (2006).
25. H. Kadono, N. Takai, and T. Asakura, "New common-path phase shifting interferometer using a polarization technique," *Appl. Opt.* **26**, 898-904 (1987).
26. Ch. S. Anderson, "Fringe visibility, irradiance, and accuracy in common path interferometers for visualization of phase disturbances," *Appl. Opt.* **34**, 7474-7485 (1995).
27. J. Glückstad and P. C. Mogensén, "Optimal phase contrast in common-path interferometry," *Appl. Opt.* **40**, 268-282 (2001).
28. C. G. Teviño-Palacios, M. D. Iturbe-Castillo, D. Sánchez-de-la-Llave, R. Ramos-García, and L. I. Olivós-Pérez, "Nonlinear common-path interferometer: an image processor," *Appl. Opt.* **42**, 5091-5095 (2003).
29. V. Arrizón and D. Sánchez-de-la-Llave, "Common-path interferometry with one-dimensional periodic filters," *Opt. Lett.* **29**, 141-143 (2004).

## 1. Introduction

Over the years, there had been many attempts to improve the resolving power of optical imaging systems beyond the Rayleigh resolution limit but all of them have involved severe modifications of the physical imaging system and often time consuming post processing algorithms. In principle, the numerical aperture (NA) and the wavelength of the illumination light determine the diffraction cutoff frequency of optical imaging systems, up to a maximum resolution of  $\lambda/2$ . This limit can only be surpassed by coupling evanescent waves, as in near field microscopy [1], or by using strong non-linearities at subwavelength scale [2]. A conventional optical system acts as a low pass filter for spatial frequencies and the image is band limited in the frequency domain. One can improve the resolution limit using larger NA aperture optical systems, but this procedure is costly and is not always possible (for example when large field or long working distance is required). In this sense, many methods have been applied to produce synthetic aperture enlargement without changes in the physical properties of the imaging system [3, 4]. All of those methods can be understood by means of the information capacity theory [5-7], which gives us an invariance theorem for the number of degrees of freedom of an optical system. This theorem states that it is not the spatial bandwidth but the information capacity of an imaging system that remains constant. Thus, it is possible to extend the spatial bandwidth by encoding-decoding the additional information onto the unused parameters of the imaging system if one knows a priori information about the object. Some examples of this a priori information are that the object may be restricted in shape [8, 9], or time [2, 10-14], polarization [15, 16] or wavelength [17]. Time multiplexing can be implemented in a variety of ways, most of them involving structured illumination, such as illumination through a physical grating [10-12] or optically generated gratings [13, 18]. Other methods [19-24] involve off-axis illumination, interferometric image plane recording and post processing stage to achieve superresolution effect with temporally restricted objects. These methods use incoherent light and the encoding of information is implicitly made on the coherence of the source [19]. As a main advantage, most objects can be considered as static in

practice, provided that their time variation is slower than the coherence time of the source. The major weakness is the need to split the input illumination beam into two beams: one used to illuminate the object in the input plane (imaging beam) and the other one is required to perform the interferometric recording onto the image plane (reference beam). Thus, dual-arm interferometric architectures like Michelson and Mach-Zehnder interferometers were used. In this paper, we present a novel technique where common-path interferometry (CPI) combined with off-axis illumination incoming from a two-dimensional (2-D) VCSEL array are used to achieve superresolution in the field of digital holographic microscopy.

The use of CPI, such as the shearing interferometer or the polarization interferometers, had been proposed mainly to retrieve the phase information [25-29]. Our proposed optical setup extends the capabilities of the CPI to the field of superresolution. This novel alternative involving the CPI implementation is applied in the superresolution techniques that use off-axis illumination to produce a synthetic aperture enlargement. Moreover, we had taken advantage of the CPI optical setup to illustrate two superresolution approaches, both of them under coherent illumination but with different resolution improvement. In the first one, a modest resolution gain factor of 2 is demonstrated while the optical setup is extremely simple and it becomes easy-to-implement in real microscopic optical systems. We will denote this first approach as “*superresolution by shared image*”. In the second approach that we present in this work, that we coin “*superresolution by CPI*”, an arbitrary resolution gain factor can be achieved. Experimental results are provided in both cases, with resolution gains by a factor of 2 and 3 respectively.

The paper is organized as follows. Section 2 gives us a mathematical analysis of the theoretical optical setup taking a  $4f$  optical processor as theoretical imaging system in order to simplify the analysis and for the general case of superresolution by CPI. Section 3 presents the experimental results for the case of superresolution by shared image as a particular case of the mathematics developed in the previous section. Section 4 provides the experimental results for the superresolution by CPI approach. Finally Section 5 concludes the paper.

## 2. Mathematical analysis of the optical setup.

The concept of the proposed method can be easily understood through the optical setup shown in Fig. 1. For simplicity, let us assume that the imaging system has a  $4f$  optical processor configuration to show the performance of the proposed approach. Thus, the input amplitude distribution is placed in the object focal plane of the first lens  $L1$  and an image of the input plane is obtained in the image focal plane of the lens  $L2$ . A circular aperture with *radius of*  $\Delta v$  is positioned in the Fourier plane of the experimental setup to limit its resolution. At the output plane, a CCD is used to record the intensity distribution that is transmitted through the imaging system. Light, coming from the 2-D VCSEL array passes through a collimation lens  $L_c$  and produces a set of parallel beams with different orientations that illuminate the input plane. In the presented approach, the VCSEL elements in the 2-D array are turned on sequentially.

Two contiguous regions compose the input plane. An object, which is represented by its amplitude distribution function  $f(x,y)$ , is placed side by side with a 2-D diffraction grating having basic frequency of  $\nu_0$  in both  $x$  and  $y$  directions. Without loss of generality we assume that this grating (*reference grating*) has the same number of diffraction orders the VCSEL sources in the 2-D array. Now, if we consider the light incoming from a single VCSEL source [at coordinates given by the indexes  $(k,l)$ ], a tilted and collimated beam impinges the input plane, so the amplitude distribution at this plane is

$$U_{input\ plane}^{(k,l)VCSEL}(x,y) = \left[ f(x,y) + \sum_{m,n=-N}^{+N} e^{-j2\pi\nu_0(mx+ny)} \right] \cdot \exp\{-j2\pi(\nu_k x + \nu_l y)\} \quad (1)$$

while  $(x,y)$  being the spatial coordinates,  $(m,n)$  the diffraction order of the reference grating, and  $N \times N$  the number of VCSEL sources in the 2-D source array.

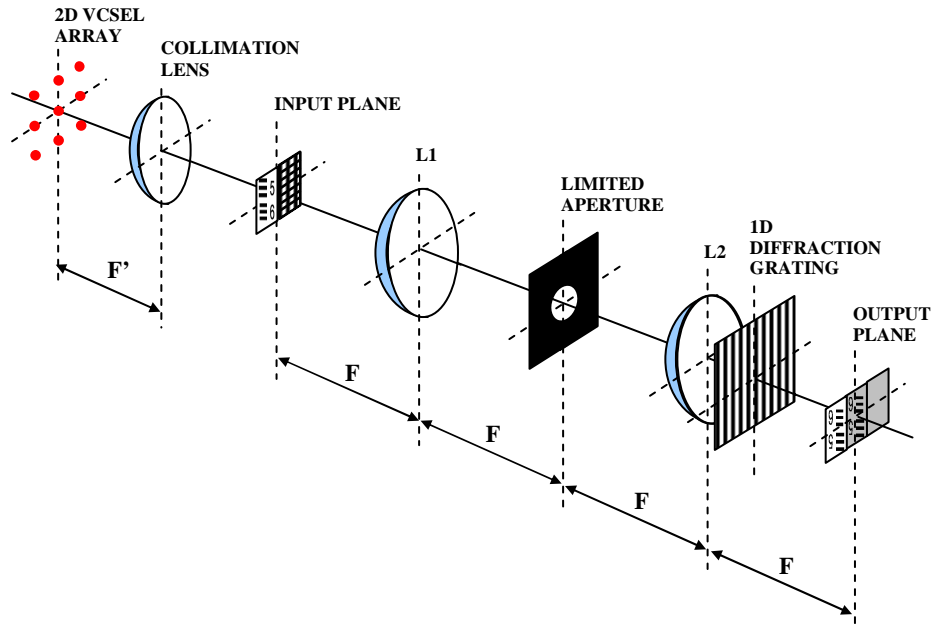


Fig. 1. Optical setup of the common-path interferometry approach used for superresolution.

In the Fourier plane of the imaging system, a Fourier transformation of the input amplitude distribution is performed and multiplied by the transmittance of the limiting circular pupil

$$U_{\text{Fourier plane}}^{(k,l)\text{VCSEL}}(u,v) = \left[ \tilde{f}(u+v_k, v+v_l) + \delta(u+v_k+mv_0, v+v_l+nv_0) \right] \text{circ}\left(\frac{\rho}{\Delta v}\right) \quad (2)$$

where  $(u,v)$  are the spatial-frequency coordinates and  $\rho$  is the polar coordinate in the frequency domain defined as  $\rho = \sqrt{u^2 + v^2}$ . At this point, two considerations are needed in order to adjust the experimental setup. On one hand, by properly adjusting the separation between the VCSEL sources in the 2-D array, the shift in the object's spectrum ensures the transmission of contiguous frequency band pass through the circular system aperture. This condition reads:

$$v_k = 2k\Delta v \text{ and } v_l = 2l\Delta v \quad (3)$$

On the other hand, the basic frequency  $v_0$  of the reference grating must be twice the radius of the circular limiting aperture ( $v_0 = 2\Delta v$ ) in order to perform the transmission of one diffraction order for each VCSEL source

$$\begin{aligned} v_k + mv_0 = 0 &\Rightarrow v_0 = 2\Delta v, \text{ if } m = -k \\ v_l + nv_0 = 0 &\Rightarrow v_0 = 2\Delta v, \text{ if } n = -l \end{aligned} \quad (4)$$

Under those conditions [(3) and (4)], Eq. (2) can be rewritten as

$$U_{\text{Fourier plane}}^{(k,l)\text{VCSEL}}(u,v) = \tilde{f}(u+2k\Delta v, v+2l\Delta v) \text{circ}\left(\frac{\rho}{\Delta v}\right) + \delta(u,v) \quad (5)$$

Then, the second lens of the  $4f$  optical processor performs another Fourier transformation and the following amplitude distribution is generated in the output plane

$$U_{Output\ plane}^{(k,l)VCSEL}(x, y) = \left[ f(-x, -y) \exp\{-j2\pi 2\Delta\nu(x+y)\} \right] \otimes disk(\Delta\nu r) + A_{m,n} \quad (6)$$

being  $r$  the polar coordinate defined as  $r = \sqrt{x^2 + y^2}$ . Note that the delta function located in the centre of the circular pupil [Eq. (5)] gives rise to a collimated beam in the image space with certain amplitude  $A_{m,n}$  coming from the  $(m,n)$  diffraction order in the reference grating and it becomes the *reference beam* of the interferometric setup.

But both terms in Eq. (6) are not overlapping because they are coming from different regions in the input plane. Thus, in order to produce the interference process between them, a second diffraction grating is placed between the lens  $L2$  and the output plane. Let us call this second diffraction grating as *imaging grating*. For simplicity, the imaging grating is chosen to be one-dimensional and it produces multiple images in the output plane with a lateral shift that depends on the  $\nu_l$  basic frequency of the imaging grating and the distance  $d'$  between the imaging grating and the output plane. This situation is depicted in Fig. 2. By means of the axial displacement of the imaging grating, the images corresponding to the uniform term and the object term [Eq (6)] can be overlapped. Then, by placing the CCD in the overlapping region, formed by the 0 and  $-1$  diffraction orders of the imaging grating (see Fig. 2), the following intensity distribution can be recorded

$$I_{output\ plane}^{(k,l)VCSEL}(x, y) = \left| \left[ f(-x, -y) \exp\{-j2\pi 2\Delta\nu(x+y)\} \right] \otimes disk(\Delta\nu r) + A_{m,n} \exp\{-j2\pi\nu_l x\} \right|^2 \quad (7)$$

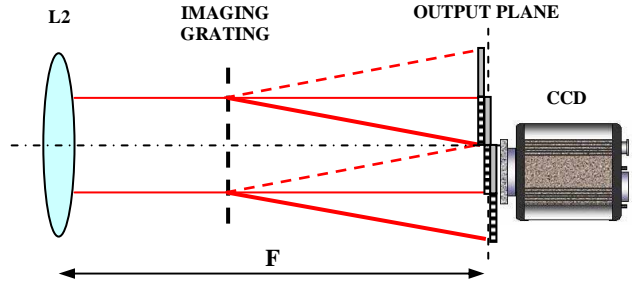


Fig. 2. Schematic sketch of the interferometric recording between the object image (horizontal grating rectangle) and the reference beam (uniform gray color rectangle).

Equation (7) provides four terms when square modulus is expanded. Let's name this four terms as:  $T_1^{(k,l)}(x, y)$ ,  $T_2^{(k,l)}(x, y)$ ,  $T_3^{(k,l)}(x, y)$  and  $T_4^{(k,l)}(x, y)$ . Once the intensity distribution is stored, we perform digitally an inverse Fourier transformation. The Fourier transform of the first term ( $\tilde{T}_1^{(k,l)}(u, v)$ ) is just a delta function centered at the origin. The second term, also centered at the origin, is the centered autocorrelation of the frequency band pass (with total width of  $4\Delta\nu$ ).

$$\tilde{T}_2^{(k,l)}(u, v) = \left[ \tilde{f}(u + 2k\Delta\nu, v + 2l\Delta\nu) \text{circ}\left(\frac{\rho}{\Delta\nu}\right) \right] * \left[ \tilde{f}(u + 2k\Delta\nu, v + 2l\Delta\nu) \text{circ}\left(\frac{\rho}{\Delta\nu}\right) \right] \quad (8)$$

where  $*$  denotes correlation.  $\tilde{T}_3^{(k,l)}(u, v)$  is the frequency band pass transmitted by the circular pupil and it is placed at the left position of the previous band pass

$$\tilde{T}_3^{(k,l)}(u, v) = (A_{m,n})^* \left[ \tilde{f}(u + 2k\Delta\nu, v + 2l\Delta\nu) \text{circ}\left(\frac{\rho}{\Delta\nu}\right) \right] \otimes \delta(u + \nu_l, v) \quad (9)$$

Taking a look on Eq. (9), one additional condition must be fulfilled: the imaging grating must have a basic frequency larger than half the size of the zero order (the correlation term has total width of  $4\Delta\nu$ ) plus half the size of the frequency band pass transmitted by the

imaging system. So, it is necessary that  $v_l \geq 3\Delta v$ . Similarly,  $\tilde{T}_4^{(k,l)}(u,v)$  is the analogous to Eq. (9) but located at the positive part of the axis.

The distribution represented by the square brackets term in Eq. (9) can be isolated and centered digitally (removing thus the delta function effect) allowing us to recover the frequency band pass transmitted by the pupil system when the  $(k,l)$  VCSEL source is used.

Then, by sequential process, every frequency band pass transmitted by the circular pupil to each  $(k,l)$  VCSEL source can be recovered and by properly placing it to its original position in the object's spectrum, the entire object's spectrum can be fully reconstructed:

$$U_{rec}(u,v) = \left[ \sum_{k,l=-N}^{+N} (A_{-k,-l})^* \tilde{f}(u+k2\Delta v, v+l2\Delta v) \cdot \text{circ}\left(\frac{\rho}{\Delta v}\right) \right] = \tilde{f}(u,v) \left[ \sum_{k,l=-N}^{+N} (A_{-k,-l})^* \text{circ}\left(\frac{\rho}{\Delta v}\right) \otimes \delta(u+k2\Delta v, v+l2\Delta v) \right] \quad (10)$$

where the term between the square brackets defines the synthetic aperture (SA) of the system

$$SA(u,v) = \sum_{k,l=-N}^{+N} (A_{-k,-l})^* \text{circ}\left(\frac{\rho}{\Delta v}\right) \otimes \delta(u+k2\Delta v, v+l2\Delta v) \quad (11)$$

Thus, except for unimportant constants, the SA generated by the suggested approach is actually the convolution of the coherent transfer function (CTF) of the system with the 2-D  $N \times N$  VCSEL array. Provided that there is a diffraction order in the reference grating for each VCSEL source in the 2-D array, any SA can be generated. Moreover, note that no assumption about the properties of  $f(x,y)$  is made, so for any complex input distribution we always will reconstruct that input. This advantage is important for applications as interferometric microscopy, three-dimensional imaging or invariant pattern recognition where phase objects play an important role.

### 3. Experimental results: superresolution by shared images.

As in the previous step showing the capabilities of the proposed superresolution method, let's take a look on a particular case where no reference grating is placed in parallel to the input object. Then, onto the CCD that is placed in the output plane, an interferometric recording is done between the object's image and a shifted version of itself due to the imaging grating. We adjust the shift between images such that the shifted image coincides with a uniform transparent region (outside the test object) that acts as reference beam in the interference process. Note that the system is indeed a simplified CPI system with only one beam splitting.

In absence of the reference grating, in order to ensure that this reference beam always has enough intensity to allow the interference process, the central part of the object's spectrum needs to be transmitted by the pupil function of the imaging lens. In other words, it is necessary that the imaging lens being able to collect light of the illumination beam. Otherwise, only diffracted frequencies will be transmitted and no reference beam could be defined in the interferometric recording. The limit to accomplish the previous condition is done by tilting angles onto the input plane equal to the NA of the imaging lens. Under this condition, the central part of the object's spectrum (the one which carries the major amount of light and contains the information for the uniform regions of the object) is transmitted for every imaging system. This particular case has been experimentally tested. In the experiments, a cross shape of  $3 \times 3$  VCSEL source had been sequentially activated. Those VCSEL sources are monochromatic with  $\lambda = 850 \text{ nm}$ . Results are provided for two cases. In the first, a Nikon microscope objective with 0.1NA is used to image a positive USAF resolution test target. In the second one, a Mitutoyo infinity corrected microscope objective with 0.14NA is used to image a negative USAF high-resolution test target. Fig. 3 shows the images obtained in both

cases. The imaging grating has a period of 80 lp/mm and it is placed appropriately in front of the CCD to perform the previously commented interferometric recording.

According to the Fig. 3(a), the resolution limit is 3.9  $\mu\text{m}$  (Group 7, Element 1, with 128 lp/mm) in the case of Nikon objective. With the Mitutoyo objective, the resolution limit is 2.8  $\mu\text{m}$  (Group 7, Element 4, with 181 lp/mm). Both experimental values match with the expected resolution according to the resolution given by  $R=\lambda/2/NA$ .

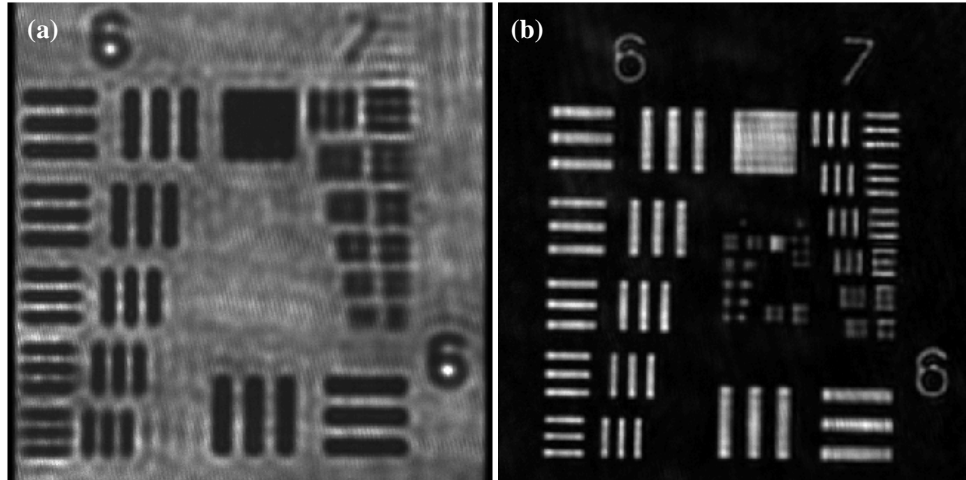


Fig. 3. Low resolution images: (a) USAF test imaged with the NIKON objective microscope (0.1NA), and (b) High resolution USAF test imaged with the MITUTOYO infinity corrected objective microscope (0.14NA).

Figure 4 shows the superresolved images for both microscope objectives when a resolution improvement factor of 2 is generated. We can see that, for the case of the Nikon objective, the overall image is resolved (2.2  $\mu\text{m}$  smallest detail size corresponding to the Group 7, Element 6) and in the Mitutoyo objective case, the resolution limit is 1.5  $\mu\text{m}$  corresponding to the Group 8, Element 3. Again these values are in agreement with the theoretical resolution limits with super resolving factor of approximately 2 for both lenses.

Although the resolution gain factor is modest (smaller than 2), the presented approach provides a simplified way to increase the resolution of a microscope objective with minimal complexity in the resulting imaging system while it is done only by taking into account coherent off-axis illumination and the common-path interferometric recording obtained by the insertion of a diffraction grating placed in front of the CCD. Moreover, when incoherent illumination is used in microscopy, the resolution is improved by factor of 2 in comparison with the coherent illumination case. With this approach, we demonstrate a method to make equal the resolution of coherent and incoherent illumination cases but taking the advantages of the coherent case (flat transfer function and possibility to recover the object's phase).

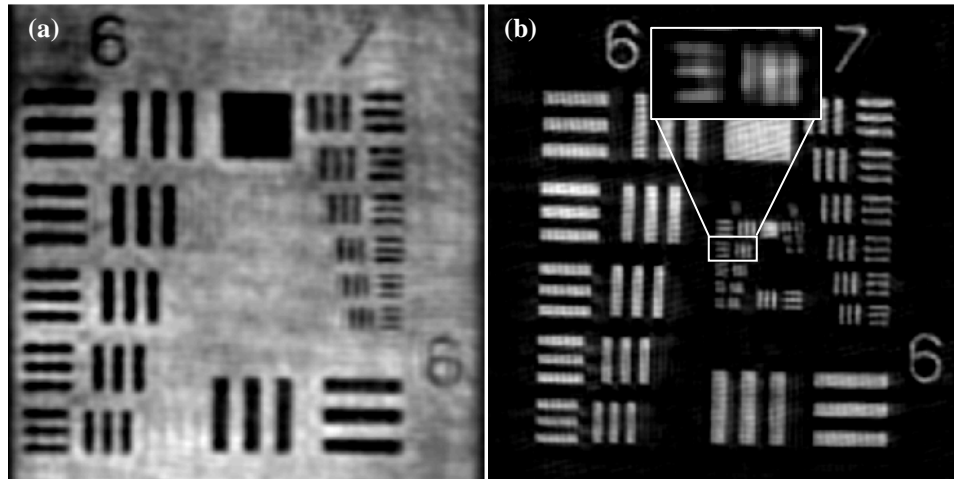


Fig. 4. Superresolved images using the presented approach to double the resolution: (a) USAF test and (b) High resolution USAF test.

#### 4. Experimental results: superresolution by common-path interferometry.

Now, the proposed superresolution method analyzed in Section 2 has been experimentally tested. In contrast to Fig. 1, the  $4f$  optical processor has been replaced (see Fig. 5) by the Mitutoyo infinity corrected microscope objective described in the previous Section. Attached to the object we place a 2-D holographic grating with a period of  $2.5 \mu\text{m}$  (reference grating). This period means that when a 20 degrees tilted collimated beam impinges on the input plane, the first diffraction order of the reference grating goes on axis. In order to obtain a tilted collimated beam, the VCSEL array is placed in the object focal plane of a collimation lens. Sequential activation of the VCSELs will provide the different tilts.

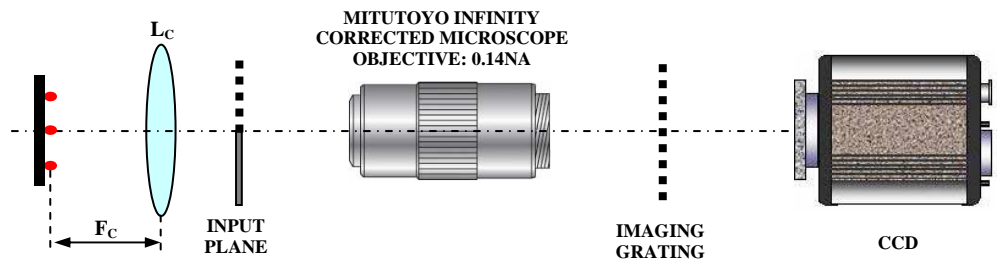


Fig. 5. Optical setup of the superresolution by common-path interferometry approach experimentally used.

As the Mitutoyo objective lens has 0.14NA, the tilt in the illumination beam should be 25 degrees in order to triple the resolution (or triple the synthetic NA), but since the reference grating we use here has a lower diffraction angle, the resolution is only improved by a factor of 2.5, approximately. Experimental results verify this assertion. Figure 6(a) shows the recorded hologram for on-axis illumination and a magnified region of the interference fringes. Figure 6(b) depicts the Fourier transform of the intensity distribution in Fig. 6(a). The interferometric recording was performed by means of a 1-D diffraction grating with a frequency of 80 lp/mm. The axial position of the grating is adjusted until the superposition of the desired terms (see Section 2) is achieved.



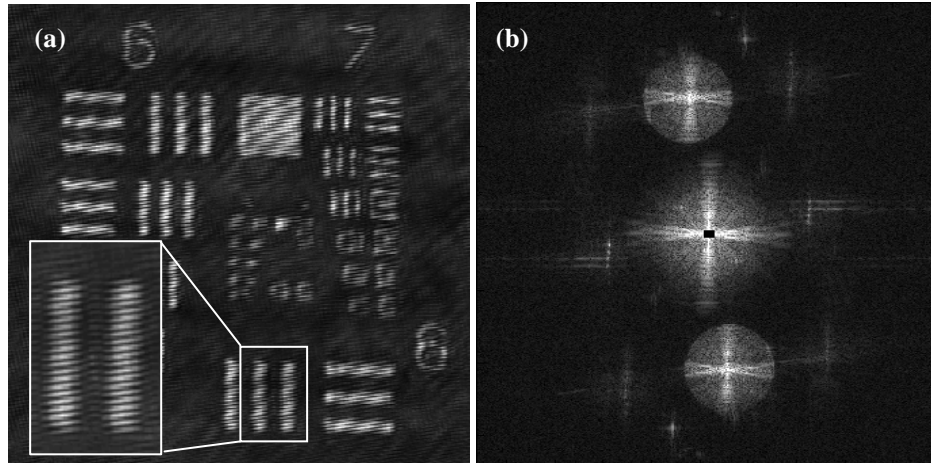


Fig. 6. (a) Recorded hologram for the on-axis illumination case, and (b) Fourier transformation of the intensity distribution presented in (a).

Figure 7 depicts the superresolved image and its spectrum (showing the SA boundary). As we can see in Fig. 7(a), the resolution limit is  $1.1 \mu\text{m}$  (Group 8, Element 6), which would correspond to a 0.38NA microscope objective.

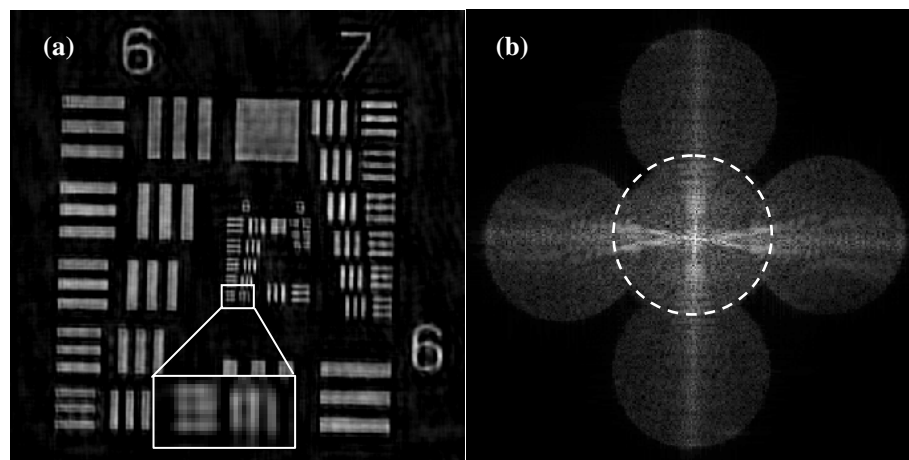


Fig. 7. Results comparison: (a) superresolved image with the presented approach, and (b) its Fourier transformation (the SA).

#### 4. Conclusion and discussion

We have proposed and demonstrated an approach for enhancing the resolution of aperture limited imaging systems based on the use of tilted illumination and common-path interferometric recording. As a main advantage of the proposed method we can point the robustness and simplicity of the system, which is more stable, relatively insensitive to vibrations and require fewer optical elements than other interferometric configurations. Both the imaging and the reference for the interferometric recording follow nearly the same optical path. Thus the instabilities of the system (mechanical or due to thermal changes on both optical paths) do not affect the obtained results. The system is based on splitting the image by means of diffraction gratings near the detection plane and combining the appropriate diffraction order of a grating set close to the object. As an additional simplification, the first grating can be dropped, although then the gain in resolution is limited to a factor of 2.

The shift in the object spectrum that permits the pass of lateral band-passes through the lens is performed by illuminating with an array of coherent sources that are incoherent one with each other. We use for this purpose a VCSEL array that allows recording each band-pass in a short time due to its high optical power per every emitter. Additionally, the associated digital processing to build the superresolved image is simple and fast, as it only requires simple and linear operations.

Any of the two proposed methods are simple to implement by straight-forward modifications of the object's illumination module and by adding an element near the detector plane. Thus, they can be easily integrated in any conventional microscope.

### **Acknowledgments**

This work was supported by FEDER funds and the Spanish Ministerio de Ciencia y Tecnología under the project BFM2001-3004 and the Agencia Valenciana de Ciencia y Tecnología (AVCT), project GRUPOS03/117.